JOURNAL OF GEOPHYSICAL RESEARCH, VOL. 112, C12009, doi:10.1029/2006JC004015, 2007

An evaluation of the thermal properties and albedo of a macrotidal flat

Tae-Wan Kim,[1] Yang-Ki Cho,[1] and Edward P. Dever[2]

Received 13 November 2006; revised 31 July 2007; accepted 10 August 2007; published 19 December 2007.

[1] The thermal properties of sediment and the albedo are critical in calculating the heat flux of a tidal flat. However, they are not well known because of the difficulties of sampling and observing tidal flats. We use extensive field observations of a macrotidal flat on the western coast of Korea to determine its sediment heat capacity and albedo. The estimated heat capacity of the upper 0.1 m is 3.65×10^6 J m^{-3} K^{-1} with a water content of 70%. Heat capacity decreases with depth to 2.96×10^6 J m^{-3} K^{-1} at 0.4 m depth. Estimated thermal diffusivities are $0.47–0.63 \times 10^{-6}$ m^2 s^{-1} and $0.38–0.64 \times 10^{-6}$ m^2 s^{-1} in spring and summer, respectively. The calculated albedo is a strong function of the solar altitude and the atmospheric transmittance. Atmospheric transmittance is especially important to the albedo when the solar altitude is low. Seasonal mean albedos are 0.13 and 0.15 in spring and summer, respectively. The heat capacity and albedo values obtained above were verified by using them to make independent heat flux estimates at other stations. Estimates based on heat capacity were correlated to albedo-based heat flux estimates with an r^2 greater than 0.7.

Citation: Kim, T.-W., Y.-K. Cho, and E. P. Dever (2007), An evaluation of the thermal properties and albedo of a macrotidal flat, *J. Geophys. Res.*, *112*, C12009, doi:10.1029/2006JC004015.

1. Introduction

[2] Tidal flats are alternately exposed and inundated by the tides. Tidal flat heat content changes that occur during exposure lead to heat exchange with surrounding seawater during inundation [*Cho et al.*, 2005]. Sea surface temperature may in turn influence local ecosystems and weather. Accurate estimation of heat exchange between the air, tidal flats and seawater is essential to understanding biological and physical systems in coastal regions with large tidal flats [*Guarini et al.*, 1997].

[3] The heat exchange between tidal flats and seawater or air can be estimated from the heat content change in the tidal flat [*Guarini et al.*, 1997]. The heat content change in the tidal flat depends on thermal properties of the sediment and the change in sediment temperature by the external forces like meteorological factors and seawater temperature. The effect of external forces on the sediment temperature in tidal flat has been extensively studied [*Harrison and Phizacklea*, 1985; *Harrison*, 1985; *Vugts and Zimmerman*, 1985]. In contrast, our understanding of sediment thermal properties is lower due to the difficulties of making observations there.

[4] The vertical propagation of heat in the sediment is governed by thermal characteristics like volumetric heat capacity, thermal conductivity and thermal diffusivity [*Harrison and Phizacklea*, 1987a, 1987b]. The thermal properties of sediments are fundamentally affected by mineral composition and relative ratio of solid, water and air [*Campbell*, 1985; *Harrison and Phizacklea*, 1987b; *Harrison and Morrison*, 1993].

[5] The thermal properties of sediments in tidal flats have been studied using several different methods. Researchers have commonly estimated thermal diffusivity from the amplitude difference of sediment temperature fluctuations between layers [*Harrison*, 1985; *Vugts and Zimmerman*, 1985; *Harrison and Phizacklea*, 1985; *Piccolo et al.*, 1993]. *Guarini et al.* [1997] estimated the volumetric heat capacity of soils in sediment by comparing the predicted and the observed surface sediment temperatures. In contrast to the previous methods of estimating thermal properties in tidal flat sediment, *Campbell and Norman* [1998] calculated the volumetric heat capacity by the weighted sum of the heat capacities of the soil constituents in land-soil.

[6] The solar radiation is the most important atmospheric forcing of sediment temperature when tidal flats are exposed. Therefore a precise albedo is necessary to estimate accurately the amount of heat exchange between air and tidal flat. During daytime exposure, the tidal flat albedo changes strongly as a function of the exposure by the tidal cycle and the atmospheric transmittance. Despite this, previous works have used a fixed albedo in calculating the heat exchange between air and tidal flat, because there was no detailed information on the tidal flat albedo [*Guarini et al.*, 1997].

[7] In this study, we calculate the volumetric heat capacity of the sediment in a tidal flat using a method which has been widely applied to land soil. We estimate the thermal

[1]Faculty of Earth System and Environmental Sciences, Chonnam National University, Gwangju, South Korea.
[2]College of Oceanic and Atmospheric Sciences, Oregon State University, Corvallis, Oregon, USA.

0148-0227/07/2006JC004015$09.00

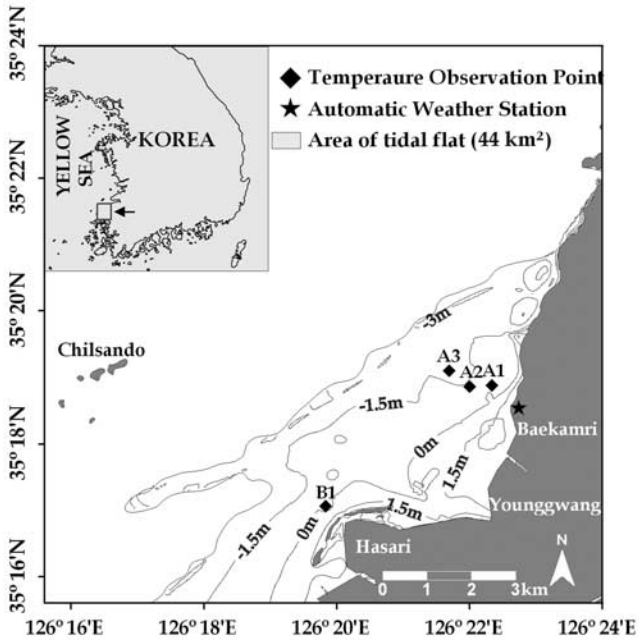

Figure 1. Study area in the Baeksu intertidal flat, southwestern coast of Korea. Numbers represent relative height to mean sea level.

diffusivity of the tidal flat sediment from the observed sediment temperature. Further, we evaluate the albedo for tidal flat area. The results are verified by comparing the heat flow into the sediment with the net heat exchange between the sediment and air.

2. Temperature Measurement in Tidal Flats

[8] The Baeksu tidal flat is a macrotidal flat off the western coast of Korea. The tidal flat trends from northeast to southwest. It is 8–10 km in length and 4–6 km in width (Figure 1), Tides are principally semidiurnal with a mean spring tidal range of 5.4 m and a mean neap tidal range of 2.4 m. The surface sediment at station A1 is composed of approximately 7% sand, 67% silt and 26% clay by dry weight [*Yang*, 2000]. Most of the sediments are spatially uniform silty clay except at some patches. The tidal flat is saturated by water due to its fine sediment and the gentle slope of the surface during the exposure. While the study site A1 is representative of the tidal flat, some patches with coarser texture may not be saturated.

[9] The sediment temperatures were measured at six different levels (−2, −5, −10, −20, −30 and −40 cm) at four stations with water temperature measurements 5 cm above the tidal flat. Measurements were continuously made for 45 d in each season (Figure 2a). The temperature measurements were made using Onset Computer Corporation HOBO temperature loggers at 3 min intervals. These instruments have a resolution of 0.02°C, with an accuracy of 0.2°C. The mean slope along the observation line is about 0.09° (Figure 2b). The exposure time ratio, defined as the ratio of the relative exposure time to that of the total observation time, is approximately 50% at station A1 and B1. Sea level data collected at a standard tidal station 10 km to the north were used to calculate the exposure times for each station. Sea level data were also recorded at a station 1.2 km west of station A3, which were used to calculate the relative variations between the tidal station and the stations in our study. The exposure time ratio decreases offshore, reaching approximately 23% at station A3. Some data were bad due to erosion of the tidal flat by waves generated by wind storms during tidal inundation. Data taken at offshore stations were not suitable for calculating the albedo due to their short exposure time. Solar radiation, wind velocity and direction, air temperature, air pressure, and relative humidity were measured by an automated weather station (AWS) installed at a station near the coast. All data were averaged to 30 min intervals for analysis.

[10] Figure 3 shows sediment temperatures, tides and solar radiation at station A1 during each season. The sediment temperature changes mainly due to the solar radiation and tides. The tidal flats were exposed during midday during the early observation period. The exposure time started 48 min later each day due to the dominant M_2 tide (12 h and 24 min period). The solar radiance peaks near noon, and is zero during night. Thus the daily cycle of the sediment temperature is likely to be complex since the frequencies of solar radiation and tidal height were slightly different.

[11] Sediment temperature also exhibits seasonal variation. The maximum surface sediment temperature is higher than 28°C in spring. During nighttime tidal exposure, the sediment temperatures dropped significantly. The temperature variability in summer was similar to that in spring. In autumn, the amplitude of the temperature wave decreases.

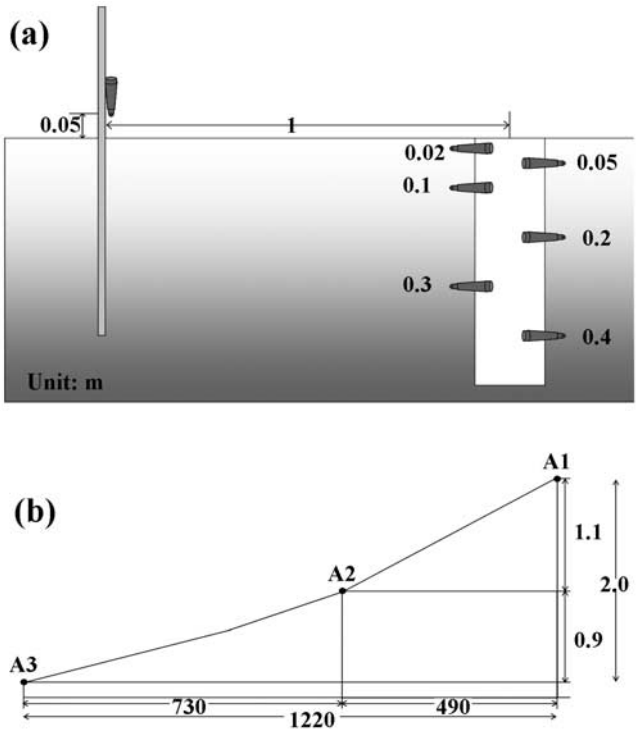

Figure 2. (a) Schematic of the sediment temperature observation in the tidal flat. (b) Distance and vertical height between the stations in Baeksu tidal flat along observation line A.

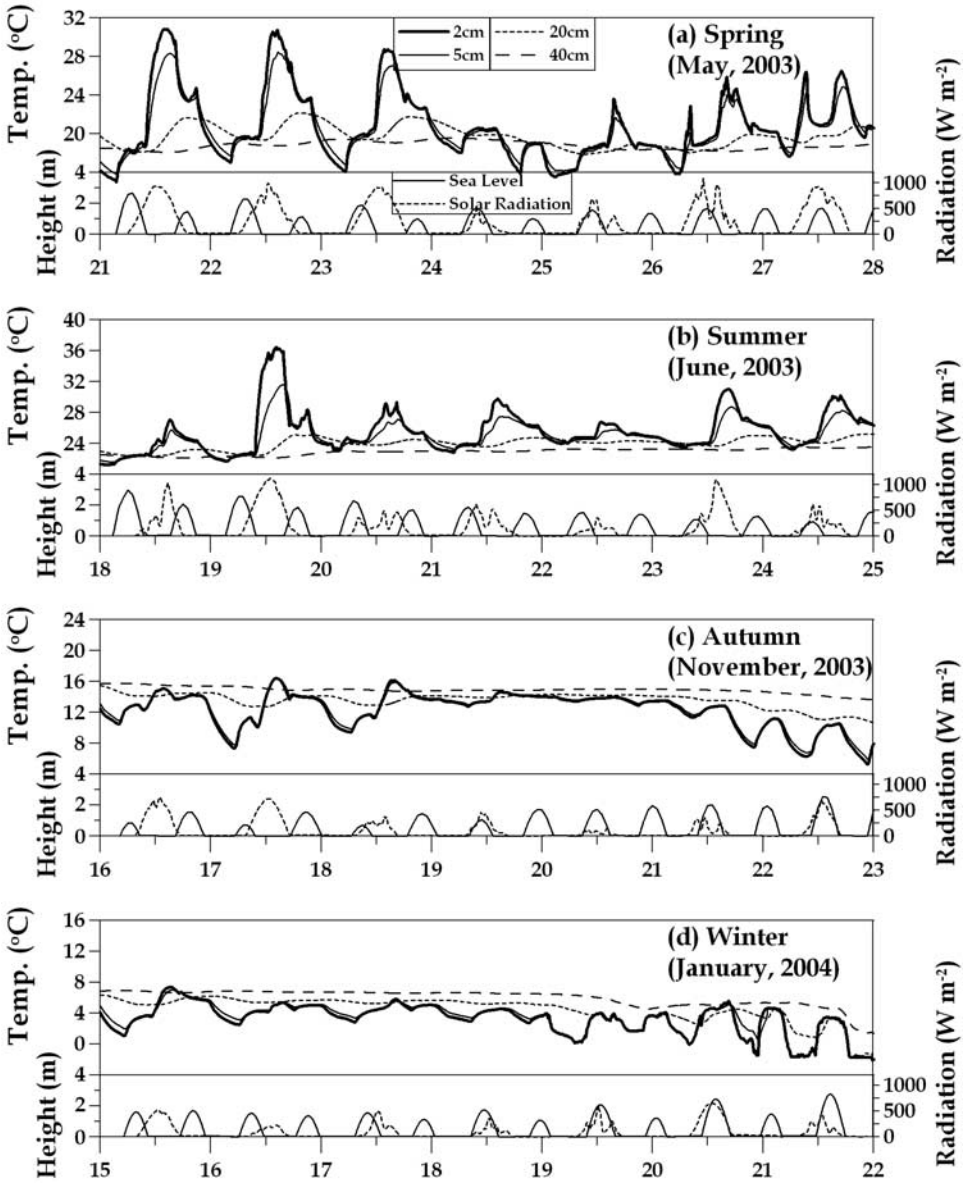

Figure 3. Temporal variations in (top) the sediment temperatures and (bottom) sea level (solid line) at station 1 and the solar radiation (dotted line) in spring.

The temperature decreases slightly during nighttime exposure and increases little during daytime exposures. Temperature variability in winter was similar to that in autumn. In all seasons, the amplitude of the sediment temperature cycle decreases with depth.

3. Evaluation of Thermal Properties of Sediment in Tidal Flat

3.1. Volumetric Heat Capacity Formulas

[12] The parameters representing thermal properties of sediment in tidal flats have been determined by different methods and formulas [e.g., *Harrison*, 1985; *Harrison and Phizacklea*, 1985; *Vugts and Zimmerman*, 1985; *Piccolo et al.*, 1993; *Guarini et al.*, 1997]. Here, we review briefly some previous methods used not only for tidal flat sediments but also for land soils where a greater number of studies have been conducted. We use the land-based parameterization to develop an improved thermal parameterization for tidal flats.

[13] *Harrison and Phizacklea* [1985] calculated sediment thermal conductivity (λ) using a Lee's disc apparatus in laboratory. They calculated thermal diffusivity (κ) from equation (1) using a purpose-built device measuring temperature variation in time:

$$\kappa = \frac{\pi}{P}\frac{(z_1 - z_2)^2}{[\ln(A_1/A_2)]^2}, \quad (1)$$

where A_1 and A_2 are amplitudes of the sediment temperature sinusoidal waves at depths z_1 and z_2, and P is the period of oscillation (12 h). Along with the calculated values of λ and

Table 1. Overview of Previous Research Regarding the Thermal Properties of Tidal Flat Sediment

Study Site	Source	Observation Depth, cm	Composition of Sediment	Water Content θ, %	Volumetric Heat Capacity C_S, 10^6 J m^{-3} K^{-1}	Thermal Diffusivity κ, 10^6 m^2 s^{-1}	Thermal Conductivity λ, W m^{-1} K^{-1}
Chichester Harbour West Sussex, England	*Harrison* [1985]	0–26.5	muddy flat	–	2.0[a]	0.41[b]	0.82[c]
Dutch Wadden Sea, Mok bay	*Vugts and Zimmerman* [1985]	3	muddy sand flat	40	2.93[a]	1.06[b]	3.11[c]
Forth estuary, Scotland	*Harrison and Phizacklea* [1985]	0–10	4% organic matter, 16% sand, 80% silt and clay	70	1.87[a]	0.47[d]	0.88[e]
Minas basin, bay of Fundy, Canada	*Piccolo et al.* [1993]	5	51.9% silt, 35.7% sand, low clay content	40	–	0.41[b]	–
Marennes-Oleron Bay	*Guarini et al.* [1997]	1	muddy flat	55%	1.65[f]	0.48[a]	0.80[c]

[a]Calculated by equation (2) using the two others thermal property parameters.
[b]Calculated by equation (1) using the in situ sediment temperature.
[c]Quoted from the previous study.
[d]Calculated by equation (1) using the observed sediment temperature in laboratory.
[e]Determined using a Lee's disc apparatus.
[f]Estimated by minimization of the sum differences between air-sediment interface heat flux and the quantity of heat change in the sediment during exposure.

κ, they determined volumetric heat capacity (C_S) from the following relationship:

$$C_S = \frac{\lambda}{\kappa}. \quad (2)$$

[14] Later, *Harrison* [1985] determined κ from equation (1) using in situ (Chichester Harbour tidal flat) vertical sediment temperature measurements. Because of its simplicity, equation (1) has been commonly used for tidal flat sediments in order to calculate κ under the assumption that in situ temperature varies as a sinusoidal function of time.

[15] Thermal properties of tidal flats reported by previous researchers are summarized in Table 1. Despite different water content and sediment composition in sediments, the calculated κ and λ are 0.41–0.48 $\times$ 10^{-6} m^2 s^{-1} and 0.80–0.88 W m^{-1} K^{-1}, respectively, except for those by *Vugts and Zimmerman* [1985]. It should be noted that most studies listed in Table 1 (except for *Harrison and Phizacklea* [1985]) measured only one parameter (κ or λ) and then estimated heat capacity, with the other thermal property taken from references. However, in situ temperature does not vary sinusoidally in a simple sine curve as they assumed but changes in a more complex way determined by the combination of tidal flat exposure time, daytime and solar radiation [*Harrison and Morrison*, 1993; *Cho et al.*, 2005]. *Guarini et al.* [1997] used a deterministic mud surface temperature model to calculate C_S by minimizing the differences between the air-sediment surface heat flux and the sediment heat content change during exposure.

[16] Alternately, the C_S of tidal flat sediment can be expressed as the weighted sum of the heat capacities of the soil constituents as given for land sediment by *Campbell and Norman* [1998]:

$$C_S = \rho_m \nu_m c_m + \rho_w c_w \theta, \quad (3)$$

where ρ_m and ρ_w are the solid particle density and water density (1.024 g cm^{-3}), respectively, and c_m and c_w are the specific heat capacities of the solid and of water, respectively; ν_m and θ are volume fractions of solid and water, respectively. Many researchers [*Ochsner et al.*, 2001; *Bristow*, 1998; *Abu-Hamdeh*, 2003] have verified equation (3) based on observations.

3.2. Volumetric Heat Capacity Calculation

[17] Use of equation (3) in tidal flats has two advantages, as compared to older, simpler methods. First, the method can be used to calculate C_S without information on κ and λ. Second, the method can be used to calculate C_S from the physical properties of sediment (bulk density of sediment and volume fraction of solid and water), without information on the sediment temperature. The second advantage is particularly useful since sediment temperature changes rapidly due to varying atmospheric conditions and seawater temperature. Use of equation (3) also avoids the possibility of temperature measurement errors propagating into the estimation of C_S.

[18] In order to estimate the C_S of sediment in our study area, we sampled sediment at each level using acrylic pipes 10 cm in length and 4.4 cm in diameter. The sampled sediments are well sealed to retain their water content during transport from the field to laboratory. Sediment particle density and water content were analyzed by the pycnometer method [*Blake and Hartge*, 1986]. Water content, defined as the volume fraction of water, is 71% at the upper 0.05 m depth and 30% at 0.45 m depth. Mean solid particle density is 2.73 g cm^{-3}.

[19] Sediment composition in the study area is similar to the silt clay loam which is used in a study of properties by *Ochsner et al.* [2001]. Thus we adopted their values of the solid heat capacity and calculated the vertical C_S in each layer. The resulting C_S ranged from 2.96–3.65 $\times$ 10^6 J m^{-3} K^{-1} depending on the water content (Table 2).

[20] Calculated volumetric heat capacities in our study are higher than those of some previous studies (1.65–2.93 $\times$ 10^6 J m^{-3} K^{-1}) in tidal flats (see Table 1). Since the volumetric heat capacity of water is 4.17 $\times$ 10^6 J m^{-3} K^{-1}, it seems natural that the volumetric heat capacity of sediment containing a large proportion of water (maximum 70%) is close to the volumetric heat capacity of water. However, the volumetric heat capacities from past studies (1.65–2.93 $\times$ 10^6 J m^{-3} K^{-1} in Table 1) are small in spite

Table 2. Physical Characteristics of the Sediment With Depth at Station A1

Depth, cm	Wet Weight, g	Dry Weight, g	Water Weight, g	Solid Volume, cm^3	Particle Density, g/cm^3	Volumetric Water Content, %	Volumetric Heat Capacity, 10^6 J m^{-3} K^{-1}
0∼10	225.10	116.90	108.20	43.85	2.67	71.16	3.65
10∼20	286.20	209.00	77.20	74.85	2.79	50.77	3.31
20∼30	299.20	232.70	66.50	85.55	2.72	43.74	3.20
30∼40	306.90	247.10	59.80	92.25	2.68	39.33	3.14
40∼50	339.20	292.60	46.60	105.65	2.78	30.65	2.96

of the large volume of water (40–70%), especially considering the volumetric heat capacity of sediment solid to be 2.0–2.5 $\times$ 10^6 J m^{-3} K^{-1} [*Ochsner et al.*, 2001]. The smaller historical estimates of heat capacity may be caused by the sediment porosity. If there is a large volume fraction of air in sediment, the volumetric heat capacity of sediment becomes small due to the minimal heat capacity (0.0012 $\times$ 10^6 J m^{-3} K^{-1}) of the air in the sediment.

3.3. Calculation of Thermal Diffusivity

[21] The thermal diffusivity (κ) of the sediment is determined by the ratio of λ and C_S which depend on the water and air content of the sediment, sediment composition, and density of sediment [*Ochsner et al.*, 2001]. *Ochsner et al.* [2001] showed a good correlation between κ and volume fraction of solids in soil.

[22] The κ of sediment can be calculated from observed sediment temperature, following the one-dimensional heat conduction equation of *Horton et al.* [1983]:

$$\frac{\partial T}{\partial t} = \kappa \frac{\partial^2 T}{\partial z^2}, \tag{4}$$

where T is sediment temperature in a layer with thickness z. In order to calculate the thermal diffusivities in each layer from equation (4), the sediment temperature profile was calculated every 5 cm using a polynomial interpolation of the observed sediment temperature profile at station A1 in

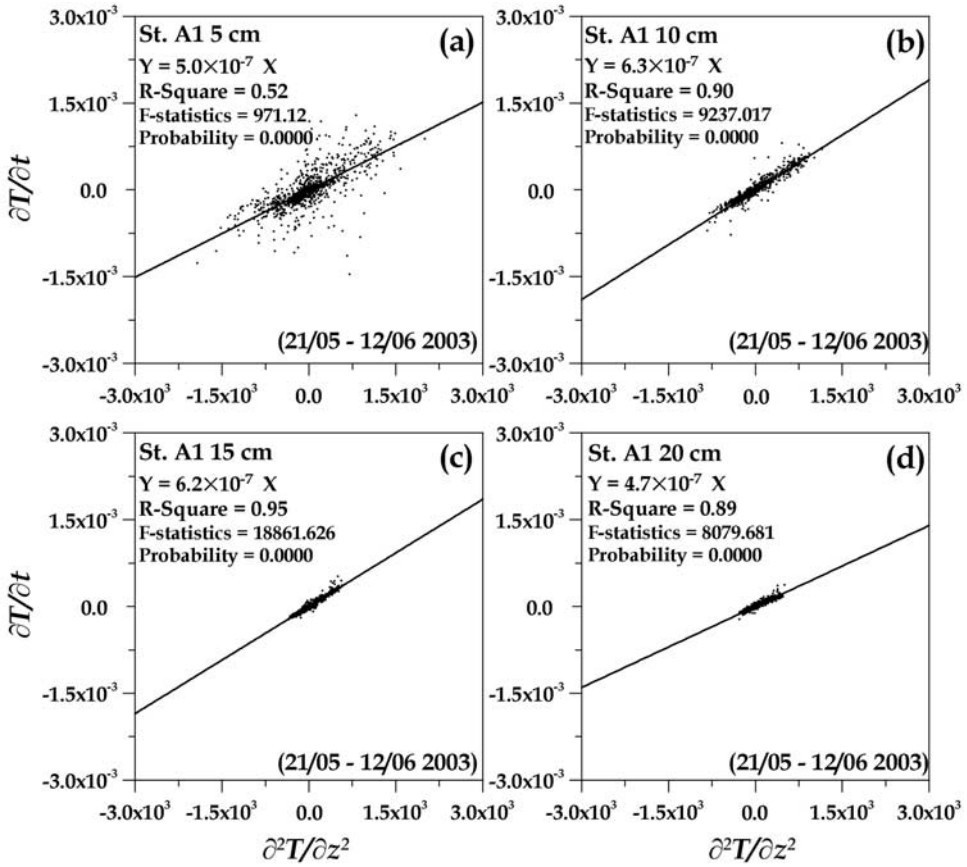

Figure 4. Thermal diffusivities in (a) 5 cm, (b) 10 cm, (c) 15 cm, and (d) 20 cm depths at station A1 in spring 2003. The x axis is the difference of the vertical temperature gradient in sediment ($\partial^2 T/\partial z^2$) and the y axis is the change rate of the temperature according to the time ($\partial T/\partial t$). The slopes represent the thermal diffusivity.

Table 3. Correlations Between the Vertical Temperature Gradient ($\partial^2T/\partial z^2$) and Temporal Temperature Change ($\partial T/\partial t$) in Sediment[a]

	28 May to 12 June 2003 (Station B1)				21 July to 13 August 2003 (Station A1)			
Layer	y, $\times 10^{-7}$	R^2	F Statistics	Probability	y, $\times 10^{-7}$ x	R^2	F Statistics	Probability
5 cm	6.1 x	0.54	807.485	0.0000	3.8	0.79	3,940.926	0.0000
10 cm	6.5 x	0.94	10,514.530	0.0000	5.0	0.94	18,324.460	0.0000
15 cm	6.6 x	0.96	16,624.266	0.0000	6.4	0.94	15,247.456	0.0000
20 cm	7.1 x	0.88	4,829.346	0.0000	4.0	0.70	2,433.892	0.0000

[a]The slopes represent the thermal diffusivity.

spring; κ can then be estimated from the slope of the fitted lines (Figure 4). The temperature change with the time ($\partial T/\partial t$) and the second derivative of the sediment temperature profile ($\partial^2T/\partial z^2$) in 5, 10, 15, and 20 cm depths are calculated from the measured sediment temperature in spring (Figures 4a, 4b, 4c, and 4d). The calculated values of $\partial T/\partial t$ and $\partial^2T/\partial z^2$ are the largest at 5 cm depth and decrease with depth. The evaluated thermal diffusivities from the fitted lines in Figure 4 are $0.47–0.63 \times 10^{-6}$ m^2 s^{-1} in spring. Table 3 shows the temporal and spatial variability of the thermal diffusivities using same method. It shows thermal diffusivities of each layer at station B1 in spring and station A1 in summer. The thermal diffusivities are $0.38–0.64 \times 10^{-6}$ m^2 s^{-1} in summer and $0.61–0.68 \times 10^{-6}$ m^2 s^{-1} at station B1 whose exposure ratio is similar to station A1. Our evaluated sediment thermal diffusivities are comparable to those of previous studies in tidal flats (Table 1).

[23] The thermal conductivity of the sediment can be estimated using the volumetric heat capacity and the thermal diffusivity from equation (2). *Ochsner et al.* [2001] showed an inverse correlation between the thermal conductivity and volume fraction of air in soil. The estimated thermal conductivity is 1.83 W m^{-1} K^{-1} using the volumetric heat capacity of 0–10 cm layer and the thermal diffusivity of the 5 cm layer at station A1 in spring, 2003. Table 4 shows the temporal and spatial variability of the thermal conductivity at 5 cm and 15 cm. The temporal and spatial variability of the thermal conductivities are 1.38–2.23 W m^{-1} K^{-1} at 5 cm layer and 2.05–2.18 W m^{-1} K^{-1} at 15 cm. These values are larger than those of most previous results (Table 1) but smaller than that proposed by *Vugts and Zimmerman* [1985].

4. Calculation of Heat Flux in Tidal Flat

[24] The heat flow into the sediment (Q_g) defined by *Harrison* [1985] is calculated based on the temperature change in each layer and the vertical temperature gradient, assuming horizontally homogeneous temperature. Under this assumption,

$$Q_g = C_S \frac{\Delta T}{\Delta t}\Delta z + \lambda \frac{\Delta T}{\Delta z}, \tag{5}$$

where T is the temperature in a layer with thickness Δz. The first term and the second term on the right-hand side in equation (5) represent the sediment thermal storage and thermal conductivity, respectively. Incoming solar irradiance increases the temperature of the sediment. Some of the incoming heat is diffused to the lower layer in proportion to the temperature difference between layers.

[25] Equation (5) can be expressed by

$$Q_g = \sum_{i=1}^{n} C_{Si} \frac{\Delta T_i}{\Delta t}\Delta z_i + \lambda \frac{\Delta T_{lowest}}{\Delta z_{lowest}}, \tag{6}$$

where C_{Si} is the observed volumetric heat capacity of each layer (i), $\Delta T_i\, \Delta t^{-1}$ is the temporal change of temperature in each layer with thickness Δz_i, and $\Delta T_{lowest} \Delta z_{lowest}^{-1}$ is vertical gradient of temperature at the lowest layer. There is little temperature change in the vertical below 30 cm [*Cho et al.*, 2005]. If we assume that the thermal conductivity at the 40 cm depth is 1.5 W m^{-1} K^{-1} and the maximum gradient of temperature is 9.5°C m^{-1} during 45 d based on observation, the calculated heat flux to the bottom is about 14.25 W m^{-2} which is only 4% of the heat flux at the surface (396 W m^{-2}) for the same period. The last thermal conductivity term in equation (6) is negligible when we include the layer deeper than 30 cm in this calculation.

[26] During the exposure by tide, the net heat exchange between the sediment and air may be expressed as

$$Q_{net} = Q_s - (Q_l + Q_e + Q_h), \tag{7}$$

where Q_{net} is net heat exchange between sediment and air and Q_s is incoming short-wave solar radiation. Q_l, Q_e and Q_h is long-wave radiation, latent heat transfer and sensible heat transfer from sediment surface to atmosphere, respectively.

[27] The net incoming solar radiation at the sediment surface is represented as

$$Q_s = (1 - \alpha)Q_{s0}, \tag{8}$$

where Q_{s0} is observed solar radiation at the automated weather station and α is albedo on the tidal flat sediment surface. Details of each term are explained in Appendix A.

5. Evaluation of the Albedo for Tidal Flats

[28] The sediment exchanges heat with the air at the surface during tidal flat exposure. If there is no heat source or sink in the sediment, the surface heat exchange equal the heat content change in the sediment plus the conductive

Table 4. Calculated Thermal Conductivities From the Volumetric Heat Capacities and the Thermal Diffusivities

Station	5 cm Layer, W m^{-1} K^{-1}	15 cm Layer, W m^{-1} K^{-1}
A1 (spring 2003)	1.83	2.05
B1 (spring 2003)	2.23	2.18
A1 (summer 2003)	1.39	2.12

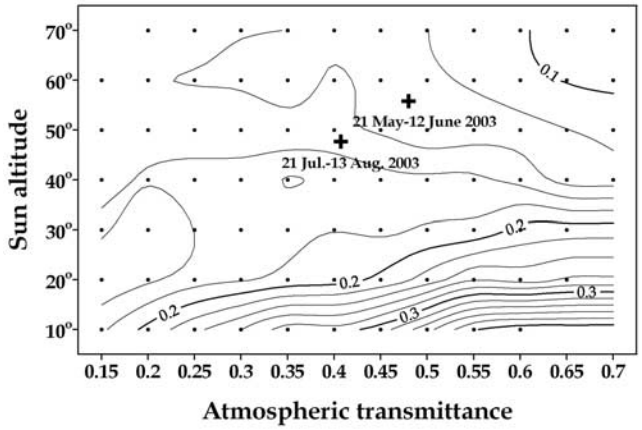

Figure 5. Calculated albedo according to the solar altitude and atmosphere transmittance at station A1 in spring and summer 2003. Albedos were average with every 10° in solar altitude and 0.05 in atmospheric transmittance. Pluses represent mean albedos for 21 May to 12 June and 21 July to 13 August 2003, respectively.

heat flux at the lowest measurement depth. The surface heat flux and the heat content in the sediment can be estimated by equations (6) and (7), respectively. In this calculation, a large, uncertain parameter is the albedo (α) in equation (8).

[29] *Guarini et al.* [1997] used a fixed albedo of 0.08 when they predicted the surface temperature of a tidal flat because there was no detailed information on α there. However, it is known that α on the sea surface is a function of atmospheric transmittance and solar altitude [*Payne*, 1972]. The incoming light to the Earth surface is divided into the direct and the scattered light. The albedo is sensitive to the solar angle only for direct light. When the atmospheric transmittance is higher than 0.6, direct light dominates and the solar angle is the major factor in determining albedo. As atmospheric transmittance decreases, the scattered light becomes stronger relative to the direct light and the solar angle becomes less important in determining albedo. Tidal flats are unique systems having characteristics of both land and water; α in the tidal flat may vary largely with the atmospheric transmittance and solar altitude. Recently, *Matthias et al.* [2000] reported that α is closely

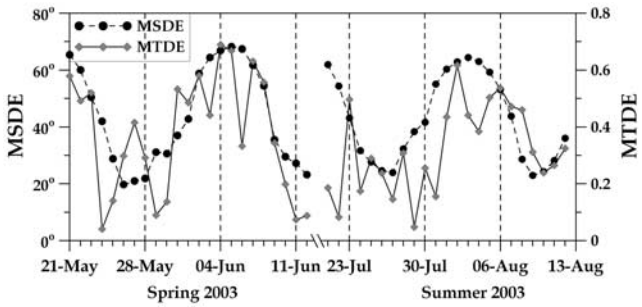

Figure 6. Variations of the daily mean solar altitude during the daytime exposure (MSDE) and the daily mean atmospheric transmittance during daytime exposure (MTDE) at station A1 during daytime exposure in spring and summer 2003.

Table 5. Variability of MADE According to MSDE and MTDE[a]

Case	Day	MSDE	MTDE	MADE
1	27 May 2003	20°	0.4	0.19
2	5 June 2003	70°	0.7	0.10
3	27 July 2003	25°	0.15	0.15
4	4 August 2003	65°	0.4	0.14

[a]MADE, daily mean albedo during the daytime exposure; MSDE, daily mean solar altitude during the daytime exposure; and MTDE, daily mean atmospheric transmittance during daytime exposure.

related to the water content of the soil; α is 0.137–0.204 for sandy soil with water content of 35% and 0.101–0.137 for muddy soil with water content of 45%.

[30] We calculated α according to the atmospheric transmittance and the solar altitude at station A1 in spring and summer. The atmospheric transmittance (T_r) is a function of the solar radiation (Q_{S0}), the solar constant (S_C : 1367 W m^{-2}), solar altitude (ϕ) and Sun-Earth radius vector (γ) [*Payne*, 1972]:

$$T_r = \frac{Q_{S0} \cdot \gamma^2}{S_C \sin(\phi)}. \tag{9}$$

[31] Combining equation (7) with (8), α on the surface of tidal flat surface can be estimated as follows:

$$\alpha = \frac{Q_{s0} - (Q_l + Q_e + Q_h) - Q_g}{Q_{s0}}, \tag{10}$$

α calculated at station A1 in spring and summer were averaged at intervals of 10° in solar altitude and 0.05 in atmospheric transmittance to figure out its relation to the solar altitude and atmospheric transmittance (Figure 5); α on the tidal flat increases rapidly with atmospheric transmittance due to the sharp increase in reflection when

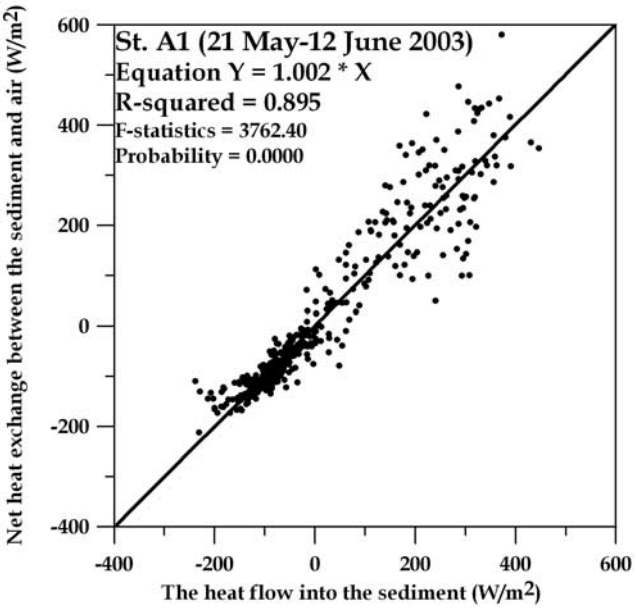

Figure 7. Correlation between sediment heat change and heat exchange through the sediment-atmosphere interface at station A1 in spring 2003.

Table 6. Correlation Between Heat Change in the Sediment and Heat Exchange Through the Sediment-Air Interface

	21 May to 12 June 2003				21 July to 13 August 2003			
Station	y	R^2	F Statistics	Probability	y	R^2	F Statistics	Probability
A1	1.002 x	0.895	3,762.400	0.0000	1.009 x	0.724	1,426.682	0.0000
A2	0.994 x	0.830	2,197.409	0.0000	1.005 x	0.769	833.145	0.0000
A3	0.998 x	0.844	708.849	0.0000	1.009 x	0.777	385.171	0.0000
B1	1.002 x	0.832	2,393.054	0.0000	0.998 x	0.790	1,845.128	0.0000

the solar altitude is low. In contrast, when the solar altitude is high, α decreases slowly with increase in atmospheric transmittance. This characteristic of calculated α on a tidal flat corresponds to that on the sea surface [*Payne*, 1972].

[32] Mean atmospheric transmittance and solar altitude during the observation period were 0.48 and 55.8° in spring and were 0.41 and 47.7° in summer. Corresponding α for those values in Figure 5 are 0.13 and 0.15 in spring and in summer, respectively. These values are greater than 0.08 which was used to calculate heat flux in tidal flat by *Guarini et al.* [1997] but are comparable to the values (0.101–0.204) reported for wet soil by *Matthias et al.* [2000].

[33] The daily mean α of the tidal flat during daytime exposure (MADE) determined by the daily mean atmospheric transmittance during daytime exposure (MTDE) and the daily mean solar altitude during the daytime exposure (MSDE) change more than those on the sea surface and land surface. MSDE changes greatly, because the exposure time varies according to the relative phase of daylight and tide (Figure 6). The MSDE is about 65° in 5 June 2003 when high water time is midday and midnight. In contrast, it is about 20° in 26 May 2003 when high water time is early morning and late afternoon. The MSDE changes with spring neap tide cycles and the daily mean solar altitude changes seasonally. We selected four cases to examine MADE variation according to the solar altitude and atmospheric transmittance (Table 5). MADE is as high as 0.19 in spring and summer 2003 in 24 May 2003 because the reflection of direct irradiation increases steeply due to low solar altitude (20°) and high atmospheric transmittance (0.4) (case 1). MADE is at its lowest, 0.10, in 5 June 2003 because the reflection of direct irradiation decreases steeply due to high solar altitude (65°) and high atmospheric transmittance (0.65) (case 2). MADE (0.15) in 27 July 2003 (case 3) is lower than case 1 because although solar altitude is similar to that of case 1, the reflection of direct irradiation is small due to low atmospheric transmittance (0.15). case 4 shows that MADE increases with decrease of atmospheric transmittance.

[34] The net heat exchange (Q_{net}) between the sediment and the air with seasonal mean α in spring and in summer were compared with the heat flow into the sediment (Q_g). Q_g and Q_{net} have good correlation at station A1 in spring (R^2 = 0.895 and slope is 1.002; Figure 7) and summer (R^2 = 0.724 and slope is 1.009; Table 6) 2003. We extended our calculation to stations A2, A3, and B1 with the α determined at station A1 (Table 6). The determination coefficient (R^2) between Q_g and Q_{net} shows a correlation more than 0.8 at four stations in spring and 0.7 in summer 2003. Data quality in other seasons was not suited to examine the correlation due to bad weather and fishing activity. The correlations at most stations were relatively poor in early morning and late afternoon since the tidal flat α change is too sensitive to the atmosphere transmittance during the low solar altitude as shown in Figure 5.

6. Conclusions

[35] Our extensive observations on tidal flat make it possible to evaluate volumetric heat capacity, thermal diffusivity and albedo. Volumetric heat capacity is largely dependent on the volume fraction of the air, water and solid in the sediment. Calculated volumetric heat capacity is the largest at the surface, 3.65×10^6 J m^{-3} K^{-1} and decreases with depth to 2.96×10^6 J m^{-3} K^{-1} at 40 cm. Thermal diffusivities of the sediment evaluated from the slope of the fitted lines of the sediment temperature time derivative ($\partial T/\partial t$) and the second vertical derivative of sediment temperature ($\partial^2 T/\partial z^2$) are $0.47–0.63 \times 10^{-6}$ m^2 s^{-1} in spring and $0.38–0.64 \times 10^{-6}$ m^2 s^{-1} in summer.

[36] The albedo changes with the solar altitude and the atmospheric transmittance. Seasonal mean albedos were 0.13 and 0.15 in spring and summer, respectively. Similarly, the daily mean solar altitude during daytime exposure showed periodicity with the neap spring tidal cycle. The daily mean albedo during the daytime exposure is highest on 24 May when the solar altitude is 20° and atmospheric transmittance is 0.4. On the other hand, it is the lowest on 5 June 2003 when the solar altitude is 65° and atmospheric transmittance is 0.65.

[37] The correlation between the heat flow into the sediment using the calculated heat capacity and the net heat exchange between the sediment and air using the calculated albedo shows a good relation at most stations. At stations having available data, the squared correlation coefficients are generally more than 0.8 in spring and 0.7 in summer. When we calculate surface heat flux of tidal flats, it is essential to use an albedo that changes with the atmosphere transmittance instead of a fixed value. The albedo changes rapidly according to the atmosphere transmittance when the solar altitude is low.

[38] The results of this study also provide information important to the understanding of heat exchange through the sediment water interface during inundation. The improved understanding of the heat flux in a tidal flat will allow us to estimate the tidal flat's role in seawater temperature variability in the coastal regime.

Appendix A

[39] The long-wave flux is given by [*May*, 1986]

$$Q_l = \left[\varepsilon\sigma T_a^4\left(0.4 - 0.05e_a^{1/2}\right) + 4\varepsilon\sigma T_a^3(T_M - T_a)\right] \cdot \left(1 - 0.75C^{3.4}\right), \quad \text{(A1)}$$

where ε is emissivity of the tidal flat sediment (0.96 [*van Bavel and Hillel*, 1976]), σ is Stefan-Boltzman constant (5.6705×10^{-8} W m^{-2} K^4), T_M is the absolute temperature (i.e., K) of the tidal surface, T_a is the absolute temperature of the atmosphere above the sediment, e_a is vapor pressure of the atmosphere above the sediment and C is amount of cloud.

[40] The sensible heat transfer on a tidal surface is given by [*Businger*, 1973; *Stathers et al.*, 1988; *Guarini et al.*, 1997]

$$Q_h = \rho_a C_{Pa} C_h (1 + U)(T_M - T_a), \tag{A2}$$

where ρ_a is density of air (1.2929 kg m^{-3}), C_{Pa} is specific heat of air at constant pressure (1003.0 J kg^{-1} K^{-1}), C_h is bulk transfer coefficient for conduction (0.0014) and U is wind speed (m s^{-1}).

[41] The latent heat transfer at the surface of sediment is given by [*Guarini et al.*, 1997]

$$\begin{aligned} Q_e &= \xi V_W, \\ V_W &= \rho_a L_V C_V (1 + U)(q_M - q_a), \\ L_V &= (2500.84 - 2.35(T_M - 273.16)) \times 10^3, \\ q_a &= \frac{0.621 P^{\vee}_{sat}}{P_{Atm} - (1 - 0.621) P^{\vee}_{sat}}, \end{aligned} \tag{A3}$$

where ξ is the water content of the tidal flat surface, L_V is the latent heat of evaporation, C_V is the bulk transfer coefficient for conduction (0.0014), U is the wind speed (m s^{-1}), q_M is the specific humidity of saturated air at water temperature [*Goff*, 1957], q_a is the specific humidity of air, $P^{\vee}_{sat}$ is the vapor pressure in saturation at interstitial water temperature, and P_{Atm} is the vapor pressure of atmosphere.

[42] The surface sediment temperature was calculated by using the sediment temperatures observed at 5 cm and 10 cm depths and the thermal diffusivity of the 5 cm layer. Then equation (4) can be approximated by a finite difference equation:

$$\frac{T_5^{n+1} - T_5^n}{\Delta t} = \kappa \frac{T_{10}^n - 2T_5^n + T_0^n}{(\Delta z)^2}, \tag{A4}$$

where n is the time interval (180 s), T_0^n is the surface temperature at nth time and Δz is the depth interval of the each layer (0.05 m) and κ is the thermal diffusivity at 5 cm depth.

[43] The surface sediment temperature T_0^n can be obtained by

$$T_0^n = 2T_5^n - T_{10}^n + \left(\frac{(\Delta z)^2}{\kappa}\right)\left(\frac{T_5^{n+1} - T_5^n}{\Delta t}\right). \tag{A5}$$

[44] **Acknowledgments.** The authors would like to thank KHNP for helping data collection in tidal flat. Y.-K. Cho was financially supported by Chonnam National University. This publication was supported by Korea Research Foundation grant funded by Korea Government (KRF-2005-070-C00142). Data analysis was supported by ARGO program of Korean Meteorological Agency.

References

Abu-Hamdeh, N. H. (2003), Thermal properties of soils as affected by density and water content, *Biosyst. Eng.*, *86*, 97–102.

Blake, G. R., and K. H. Hartge (1986), Particle density, in *Methods of Soil Analysis. Part I. Physical and Mineralogical Methods*, edited by A. Klute, pp. 377–378, Am. Soc. of Agron., Madison, Wis.

Bristow, K. L. (1998), Measurement of thermal properties and water content of unsaturated sandy soil using dual-probe heat-pulse probes, *Agric. For. Meteorol.*, *89*, 75–84.

Businger, J. A. (1973), Turbulent transfer in the atmospheric surface layer, in *Workshop on Micrometeorology*, edited by D. A. Haugen, pp. 67–100, Am. Meteorol. Soc., Boston, Mass.

Campbell, G. S. (1985), *Soil Physics With BASIC-Transport Models for Soil-Plant Systems*, 150 pp., Elsevier, New York.

Campbell, G. S., and J. M. Norman (1998), *An Introduction to Environmental Biophysics*, 286 pp., Springer, New York.

Cho, Y. K., T. W. Kim, K. W. You, L. H. Park, H. T. Moon, S. H. Lee, and Y. H. Youn (2005), Temporal and spatial variabilities in the sediment temperature on the Baeksu tidal flat, Korea, *Estuarine Coastal Shelf Sci.*, *36*, 302–308.

Goff, J. A. (1957), Saturation pressure of water on the new Kelvin temperature scale, *Trans. Am. Soc. Heat. Ventilating Eng.*, *63*, 347–354.

Guarini, J. M., G. F. Blanchard, P. Gros, and S. J. Harrison (1997), Modelling the mud surface temperature on intertidal flats to investigate the spatio-temporal dynamics of the benthic microalgal photosynthetic capacity, *Mar. Ecol. Prog. Ser.*, *153*, 25–36.

Harrison, S. J. (1985), Heat exchange in muddy intertidal sediments, Chichester Harbour, West Sussex, England, *Estuarine Coastal Shelf Sci.*, *20*, 477–490.

Harrison, S. J., and A. P. Phizacklea (1985), Seasonal changes in heat flux and heat storage in the intertidal mudflats of the Forth estuary, Scotland, *J. Climatol.*, *5*, 473–485.

Harrison, S. J., and A. P. Phizacklea (1987a), Temperature fluctuation in muddy intertidal sediments, Forth estuary, Scotland, *Estuarine Coastal Shelf Sci.*, *24*, 279–288.

Harrison, S. J., and A. P. Phizacklea (1987b), Vertical temperature gradients in muddy intertidal sediments in the Forth estuary, Scotland, *Limnol. Oceanogr.*, *32*, 954–963.

Harrison, S. J., and P. Morrison (1993), Temperature in a sandy beach under strong solar heating: Patara Beach, Turkey, *Estuarine Coastal Shelf Sci.*, *37*, 89–97.

Horton, R., P. J. Wierenga, and D. R. Nielsen (1983), Evaluation of methods for determining the apparent thermal diffusivity of soil near the surface, *Soil Sci. Soc. Am. J.*, *47*, 14–20.

Matthias, A. D., A. Fimbres, E. E. Sano, D. F. Post, L. Accioly, A. K. Batchily, and L. G. Ferreira (2000), Surface roughness effects on soil albedo, *Soil Sci. Soc. Am. J.*, *64*, 1035–1041.

May, P. W. (1986), A brief explanation of Mediterranean heat and momentum flux calculations, NORDA Code 322, Nav. Ocean Res. and Dev. Activity, NSTL Station, Miss.

Ochsner, T. E., R. Horton, and T. Ren (2001), A new perspective on soil thermal properties, *Soil Sci. Soc. Am. J.*, *65*, 1641–1647.

Payne, R. E. (1972), Albedo of the sea surface, *J. Atmos. Sci.*, *29*, 959–970.

Piccolo, M. C., G. M. E. Perillo, and G. R. Daborn (1993), Soil temperature variations on a tidal flat in Minas basin, Bay of Fundy, Canada, *Estuarine Coastal Shelf Sci.*, *35*, 345–357.

Stathers, R. J., T. A. Black, W. G. Bailey, and M. D. Novak (1988), Modeling surface energy fluxes and temperature in dry and wet bare soils, *Atmos. Ocean*, *26*, 59–73.

van Bavel, C. H. M., and D. I. Hillel (1976), Calculating potential and actual evaporation from a bare soil surface by simulation of concurrent flow of water and heat, *Agric. Meteorol.*, *17*, 453–476.

Vugts, H. F., and J. T. F. Zimmerman (1985), Heat balance of a tidal flat area, Netherlands, *J. Sea Res.*, *19*, 1–14.

Yang, B. C. (2000), Seasonal cycle of surface sediment distribution and evolution of sedimentary facies on the Baeksu intertidal flat, south western coast of Korea Peninsula, M.Sc. thesis, 147 pp., Chonnam Natl. Univ., Gwangju, South Korea.

Y.-K. Cho and T.-W. Kim, Faculty of Earth System and Environmental Sciences, Chonnam National University, Gwangju, South Korea, 500-757. (ykcho@chonnam.ac.kr)

E. P. Dever, College of Oceanic and Atmospheric Sciences, Oregon State University, 104 COAS Admin Bldg., Corvallis, OR 97331-5503, USA.